Direct Wiring of Cytochrome *c*'s Heme Unit to an Electrode: Electrochemical Studies

By: Jianjun Wei, Haiying Liu, Allison R. Dick, Hiromichi Yamamoto, Yufan He and David H. Waldeck

J. Wei, H. Y. Liu, A. R. Dick, H Yamamoto, Y. F. He, and D. H. Waldeck, "Direct wiring of cytochrome c's heme unit to an electrode: Electrochemical studies", *Journal of the American Chemical Society*, 2002, 124 (32), 9591-9599.

Abstract:

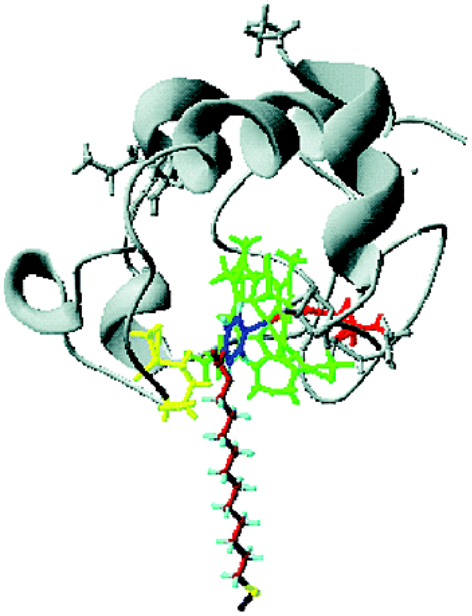

A novel strategy for the immobilization of cytochrome c on the surface of chemically modified electrodes is demonstrated and used to investigate the protein's electron-transfer kinetics. Mixed monolayer films of alkanethiols and ω-terminated alkanethiols (terminated with pyridine, imidazole, or nitrile groups that are able to ligate with the heme) are used to adsorb cytochrome *c* to the surface of gold electrodes. The use of mixed films, as opposed to pure films, allows the concentration of adsorbed cytochrome to remain dilute and ensures a higher degree of homogeneity in their environment. The adsorbed protein is studied using electrochemical methods and scanning tunneling microscopy.

Keywords: cytochrome *c* | chemically modified electrodes | electron transfer | protein

Article:

INTRODUCTION

Electron transfer reactions play a central role in biological processes, for example, photosynthesis and respiration. In addition, electron transfer processes are central to the development and operation of many biosensors and biocatalytic devices. Our understanding of electron transfer in proteins has seen great strides in recent years for both unimolecular and bimolecular processes. With the recent growth of methods to control and manipulate the surface chemistry of electrodes, heterogeneous electron transfer with biomolecules (proteins, nucleotides, etc.) should see a similar development. This work describes a strategy for immobilizing biomolecules on a chemically modified electrode through a specific interaction that provides some selectivity for the biomolecule's orientation on the surface. This strategy is realized for the binding of cytochrome *c* to the surface of chemically modified Au electrodes and should enable a range of fundamental studies on the electron-transfer kinetics.

A number of workers[1-3] have investigated the electron transfer mechanism of cytochrome *c* on electrodes. The earliest studies were reported for electrodes modified with a redox mediator through which the electrode reduces or oxidizes the cytochrome *c*. Much of this early work focused on finding systems in which the electron transfer is facile and preventing decomposition of the protein on the electrode. More recently, Miller [4] used hydroxyl-terminated alkanethiols to coat the surface of Au electrodes and found that the electron-transfer rate constant could be controlled by changing the thickness of the monolayer film; however, he did not immobilize the protein on the surface. Workers [2,3] have immobilized cytochrome *c* by electrostatic association of carboxylic acid-terminated alkanethiol monolayer films with the positively charged outer surface of the protein. These systems allow for the implementation of well-defined electrochemistry and electron transfer rate constant measurements as a function of the film thickness. However, the voltammograms obtained from such studies can display a significant degree of inhomogeneity, presumably a result of protein aggregation or a distribution of surface sites and geometries.

Most recently, cytochrome *c* was immobilized on the surface of pure monolayers of pyridine-terminated alkanethiols that had alkane chain lengths of more than six methylenes.[5] For chain lengths below six methylenes, no immobilization was observed. Presumably, the length requirement results from the need for the cytochrome to partially penetrate the film so that the pyridine moiety can interact with the heme. A large negative shift in the apparent redox potential, as compared to that observed on the carboxylic acid terminated films, was identified. Although the immobilization was robust, the electrochemical response was not very reversible, making these systems unsuitable for detailed studies of the electron-transfer mechanism.

This work demonstrates the ability to create mixed monolayer films that associate with a specific part of the protein and allow electron transfer to its redox center. Figure 1 illustrates the design of the monolayer system (panel A) and its realization for the pyridine/cytochrome *c* system (panel B). By creating mixed films of pyridine alkanethiols in a diluent of shorter chain alkanethiols, cytochrome *c* can be immobilized on the surface through association of the functionalized longer chain thiols with the heme of the cytochrome. The immobilization is achieved by an alkanethiol that is terminated with a functionality that can bind to the heme of the cytochrome. In particular,

pyridine and imidazole were found to interact strongly, and nitrile-terminated chains, more weakly. Chart 1 shows the materials used to create these three mixed-film systems. The immobilization is demonstrated by electrochemical voltammetry measurements and STM imaging of the surfaces. We further show that the voltammograms are close to ideal, which indicates well-defined sites on the surface of the electrode, allowing the electron-transfer kinetics to be characterized electrochemically. This strategy for immobilization should be applicable to many systems and should allow the use of electrochemical methods to address important issues in protein electron transfer; for example, developing structure−function relationships for the reorganization energy, quantifying the relationship between the electronic coupling and the electron-transfer mechanism, and others.

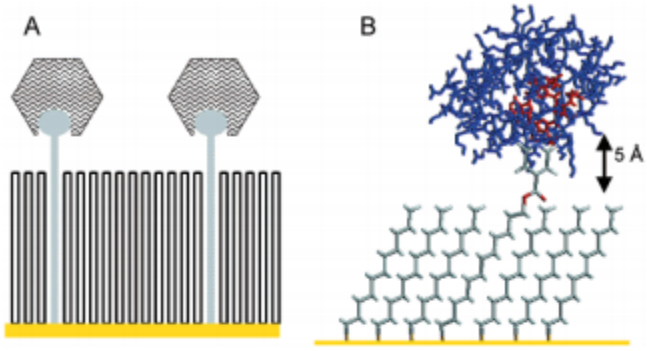

Figure 1. The schematic diagram in panel A illustrates the strategy for immobilizing a molecule on the monolayer surface through a specific binding event. The drawing in panel B illustrates the realization of this approach for immobilizing cytochrome *c* on the surface.

Chart 1

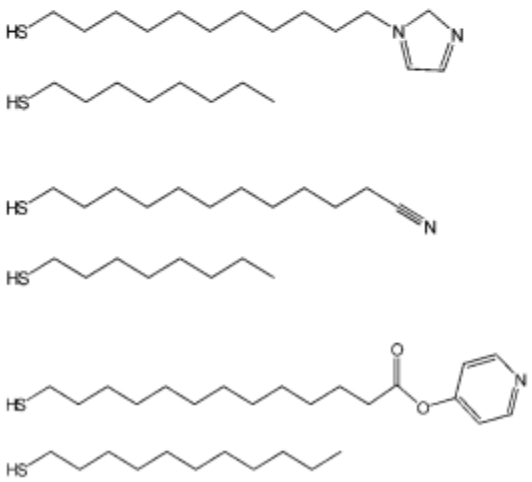

EXPERIMENTAL SECTION

Reagents and Materials. Water for experiments was purified by using a Barnstead−Nanopure system and had a resistivity of 18 MΩ·cm. 1,3-Dicyclohexylcarbodiimide, or DCC, (99%) was purchased from Alfa Aesar. 1-Octanethiol (98.5+%), 1-hexadecanethiol, and 1-undecanethiol (98+%) were purchased from Aldrich and used without further purification. Imidazole (99%), 11-bromo-1-undecanol (98%), 12-mercapto-1-dodecanol (98+%), methanolic iodine (99%),

sodium bisulfite (99%), thiourea (99+%, A.C.S. reagent), K_2CO_3 (99+%, A.C.S. reagent), NaOH (97%), and $MgSO_4$ (99%) were purchased from Aldrich. Absolute ethanol was purchased from Pharmcoproducts, Inc.

Cytochrome *c* (Sigma C 7752, from horse heart, minimum 95% based on molecular weight 12 384) was purified using a cation exchange column (CM-52, carboxymethyl-cellulose from Whatman). The purification was carried out in a cold room at 5 °C, by the reported method.[6] A 30-mg portion of cytochrome *c* was dissolved in 2 mL of 50 mM phosphate buffer solution at pH 7 (25 mM Na_2HPO_4 and 25 mM NaH_2PO_4). A small amount of $K_3Fe(CN)_6$ was added to the solution to oxidize the protein. This solution was placed onto a 1.5-cm-diameter × 30-cm-long column containing carboxymethyl cellulose (Whatman, CM-52) that was pretreated with 25 mM of the phosphate buffer. The protein was eluted with 50, 60, 70, and 80 mM phosphate buffer in a stepwise manner. The center of the last separated portion was collected. The phosphate buffer was removed from the protein using an ultrafiltration membrane (Millipore, YM10) under positive pressure. The cytochrome *c* aqueous solution was quickly frozen at −80 °C and dried in a vacuum. The purified cytochrome *c* was stored in a freezer with dry ice under an argon atmosphere until use.

Electrode Preparation. A gold wire (0.5 mm diameter,99.99%) was cleaned by reflux in nitric acid (68−70%) at 130 °C overnight and then was washed with deionized water. The tip of the gold wire was heated to form a ball of ∼0.06−0.15 cm^2 surface area. The gold ball was reheated in the flame until glowing and then quenched in deionized water. This annealing process was performed more than 15 times to make a smooth gold ball. The exposed Au wire was sealed in a glass capillary tube, and the Au ball tip was annealed and cooled in a high-purity stream of Ar gas.

Chemically modified electrodes were prepared by immersion in an ethanol solution that contained 1 mM of 1-(11-mercaptoundecyl) imidazole and 1-octanethiol (the mole ratio of 1-(11-mercaptoundecyl) imidazole to 1-octanethiol was 1:9). The electrode remained in this solution for 2−3 days to form the mixed SAM. The electrode was taken out from the solution, first rinsed with absolute ethanol, then rinsed with the supporting buffer solution (20 mM phosphate buffer pH 7), and finally dried by a stream of dry argon gas. At this stage, the electrode was used to perform characterization studies of its capacitance and voltammetric response in the buffer solution. After this characterization, the electrode was immersed in a 100 μM cytochrome *c* solution (purged with argon gas) for 30 to 60 min in order to immobilize the cytochrome on the SAM-coated electrode. These electrodes were immediately used in voltammetry studies.

After the measurements, the monolayer film was removed from the electrode by immersing it in a “piranha” solution (a mixture of 30% H_2O_2 and 98% H_2SO_4 in a 1:3 volume ratio) for 20 s and rinsed with dionized water. The surface area of the electrode was then determined by performing voltammetry in a 0.5 M KCl solution that contained 1 mM $K_3[Fe(CN)_6]$ and 1 mM $K_4[Fe(CN)_6]$. The peak current in this measurement displayed a linear relation with the square root of the scan rate.[7]

The same procedure was used to prepare the pyridine- and nitrile-terminated thiol monolayers. For the pyridine-terminated films, the 1 mM thiol solution was composed of a 1:9 mixture of 1-(12-mercaptododecyl)pyridine and 1-undecanethiol, and for the nitrile-terminated films, the 1 mM thiol solution was composed of 1-(11-mercaptoundecyl)nitrile and 1-octanethiol. For the control study in which the diluent film blocked adsorption, the SAM was composed of 1-(12-mercaptodecyl)pyridine and 1-hexadecanethiol.

Electrochemical Measurements. Cyclic voltammetry on the immobilized cytochrome *c* was carried out using an EG&G PAR-283 potentiostat, which was controlled by a Pentium computer running version 4.3 of PARC model 270 software and a GPIB board. The three- electrode cell was composed of a platinum spiral counter electrode, a Ag/AgCl (3 M NaCl) reference electrode, and the SAM-coated Au as a working electrode. The voltammetry measurements were performed in 20 mM phosphate buffer solution (pH of 7.0) under an argon atmosphere.

Impedance measurements (EIS) were performed using a VoltaLab PGZ407 universal potentiostat to determine the capacitance of the mixed SAMs before immobilization of the cytochrome *c*. The experiments were performed using a three electrode cell and a 20 mM phosphate buffer solution (pH 7.0).

STM Measurements. For the STM studies, a Au(111) facet of a single crystalline bead (prepared by Clavilier's method [8]) was used as the substrate. It was cleaned by immersion in hot piranha solution (1:3 H_2O_2 and H_2SO_4) for 1 h, followed by immersion in hot HNO_3 for 30 min. After each step, the sample was rinsed by ultrasonication in ultrapure water (>18.2 MΩ·cm) from a Barnstead−Nanopure Infinity system. The crystal was hydrogen flame-annealed, and allowed to cool to room temperature in air. The preparation of mixed SAMs of 1-(12-mercaptodecyl) pyridine and 1-undecanethiol (1:9 mole ratio) on the Au (111) bead for STM was the same as the SAMs prepared for electrochemical experiments. Two beads were put into the solution mixture for 2−3 days. One bead was rinsed with ethanol and then directly used for STM experiments, and the other bead was placed in a solution of cytochrome *c* (100 μM) for 30−60 min to immobilize the protein. This bead was rinsed with supporting buffer solution before being analyzed by STM. The STM images were obtained using a PicoScan STM system (Molecular Imaging). STM tips were cut by using 0.25-mm-diameter Pt−Ir wires (Goodfellow). All of the STM images were obtained under constant current mode at 50−100 pA and a tip−sample bias of 0.8−1.0 V.

1. Synthesis of 1-(11-Mercaptoundecyl)imidazole. The 1-(11-mercaptoundecyl) imidazole was prepared in the following manner: Imidazole (1.453 g, 21.316 mmol) and 11-bromo-1-undecanol (5.355 g, 21.316 mmol) were added together in 50 mL of dry DMF under argon atmosphere. K_2CO_3 (5.898 g, 42.676 mmol) was added to the mixed solution and stirred for 24 h at room temperature. The resulting mixture was poured into ice water and extracted with methylene chloride (350 mL) to remove DMF. The solution was dried with $MgSO_4$, filtered, concentrated, and purified by column chromatography (silica gel, chloroform) to obtain 1-(11-hydroxundecyl) imidazole. ^{1}H NMR (300 MHz) $CDCl_3$: 7.503 (s, 1H), 7.064 (s, 1H), 6.911 (s, 1H), 3.933 (t, J = 7.08, 2H), 3.64 (t, J = 6.89, 2H), 1.772 (m, 2H), 1.561 (m, 2H), 1.267 (broad, 14 H). The 1-(11-hydroxyundecyl)imidazole (3.259, 12.83 mmol) and thiourea (2.930 g, 38.492 mmol) were added to 35 mL of hydrobromic acid (48%) and refluxed for a day. The mixture was

neutralized with K_2CO_3, then NaOH was added (1.539 g, 38.492 mmol), and the solution was refluxed in an argon atmosphere for 8 h. The resulting solution was cooled to room temperature, poured into ice water, and extracted with methylene chloride. The solution was dried with $MgSO_4$, filtered, concentrated, and purified by column chromatography (silica gel, chloroform) to obtain 1-(11-mercaptoundecyl) imidazole. ^{1}H NMR (300 MHz) $CDCl_3$: 7.490 (s, 1H), 7.066 (s, 1H), 6.905 (s, 1H), 3.924 (t, *J* = 7.13, 2H), 2.522 (q, *J* = 7.47, 2H), 1.769 (m, 2H), 1.605 (m, 2H), 1.392−1.264 (broad, 15 H). EI-HRMS: Calcd., 254.18167 ($C_{14}H_{26}N_2S$). Found, 254.18215.

2. Synthesis of Bis[12-((pyridinylcarbonyl)oxy)dodecyl] disulfide.

a. Bis(12-hydroxyododecyl) disulfide. 12-Mercapto-1-dodecanol (10 mmol) was dissolved in 50 mL methanol and titrated with 0.5 M methanolic iodine until the reaction solution turned from colorless to a persistent yellow. The reaction was quenched with 10% sodium bisulfite to a colorless solution. The resulting mixture was dissolved in distilled water and extracted with CH_2Cl_2. The solvent was removed under vacuum. Purification of the resulting crude disulfide was performed by flash chromatography (CH_3Cl) to obtain the disulfide as a white solid. ^{1}H NMR (300 MHz) $CDCl_3$: δ 3.651 (q, *J* = 6.36, 4H), 2.689 (t, *J* = 7.34, 4H), 1.654 (m, 4H), 1.570 (m, 4H), 1.379−1.255 (m, 32H).

b. Bis[12-((pyridinylcarbonyl)oxy)dodecyl] disulfide. 1,3-Dicyclohexylcarbodiimide (DCC) (0.603 g, 2.92 mmol) was added to 20 mL of dichloromethane solution of bis(12-hydroxyodecyl) disulfide (0.55 g, 1.33 mmol), isonicotic acid (0.327 g, 2.66 mmol) and 4-(dimethylamino)pyridine (32 mg, 0.266 mmol) at 0 °C. After 1 h, the solution was allowed to warm to room temperature, and stirring was continued for 4 days. After removal of the precipitated dicyclohexylurea (DCU) by filtration, the solvent was removed under reduced pressure to yield a crude solid. The solid was recrystallized with ethanol to yield a white powder product. ^{1}H NMR (300 MHz) $CDCl_3$: δ 8.799 (s, 4H), 7.910 (d, *J* = 4.83, 4H), 4.369 (t, *J* = 6.60, 4H), 2.685 (t, *J* = 7.29, 4H), 1.766 (m, 4H), 1.676 (m, 4H), 1.378−1.287 (m, 32H). EI-HRMS: Calcd, 644.3702 ($C_{36}H_{56}N_2O_4S_2$). Found, 644.3682.

3. Synthesis of 12-Mercaptododecanenitrile.

a. 12-Hydroxydodecanenitrile. 11-Bromoundecan-1-ol (4.00 g, 15.923 mmol) and sodium cyanide (1.528 g, 31.84 mmol) were added to 30 mL of DMSO solution and stirred at 80 °C for 2 days. The resulting solution was extracted with methylene chloride and washed with a large amount of water to remove DMSO. The combined organic layers were washed, dried, and concentrated at reduced pressure. The crude product that resulted from evaporation of solvent was purified by column chromatography (methylene chloride) to obtain 12-hydroxydodecanenitrile. H NMR δ ($CDCl_3$): 3.626 (t, *J* = 6.60 Hz, 2H), 2.332 (t, *J* = 7.02 Hz, 2H), 1.650 (m, 2H), 1.558 (m, 2H), 1.435 (m, 2H), 1.281−1.208 (broad, 12H).

b. 12-Bromdodecanenitrile. 12-Hydroxydodecanenitrile (1.20 g, 6.09 mmol) was dissolved in 30 mL of dry ethyl ether and cooled to −10 °C. Subsequently, 0.6 mL of PBr_3 was added to the solution and stirred at room temperature for 3 days. The resulting solution was washed with 0.1 M Na_2CO_3 solution and pure water and extracted with ethyl ether. The combined organic layers were washed, dried, and concentrated at reduced pressure. The crude product that resulted from

evaporation of solvent was purified by column chromatography (methylene chloride) to obtain 12-bromodecanenitrile. H NMR δ ($CDCl_3$): 3.409 (t, *J* = 6.81 Hz, 2H), 2.337 (t, *J* = 7.10 Hz, 2H), 1.630 (m, 2H), 1.417 (m, 2H), 1.342 (m, 2H), 1.225−1.207 (b, 12H).

c. 12-Mercaptododecanenitrile. 12-Mercaptododecanenitrile was prepared according to a literature procedure.[9] 11-Bromoundecanenitrile (1.079 g, 3.978 mmol) and thiourea (0.899 g, 11.812 mmol) were added to 50 mL of dry ethanol and refluxed overnight under N_2 atmosphere. The solvent was removed at reduced pressure. A 50-mL portion of water containing KOH (0.662 g, 11.81 mmol) was added and refluxed for 6 h. The resulting solution was cooled to room temperature, extracted with methylene chloride, and washed with water. The combined organic layers were washed, dried, and concentrated at reduced pressure. The crude product that resulted from evaporation of solvent was purified by column chromatography (methylene chloride) to obtain 12-mercaptododecannitrile. H NMR δ ($CDCl_3$): 2.516 (q, *J* = 7.41 Hz, 2H), 2.332 (t, *J* = 7.08 Hz, 2H), 1.674 (m, 4H), 1.459−1.276 (b, 17H). EI-HRMS: Calcd., 213.1551 ($C_{12}H_{23}NS$). Found, 213.1542.

RESULTS

Structural Characterization. The thickness of the monolayer films was assessed through capacitance studies. AC impedance measurements were used to characterize the capacitance of the monolayer films, and the area of the electrode was determined in the manner described in the Experimental Section. For the pyridine system (dodecylpyridine and undecane), an average capacitance of 1.34 ± 0.17 μF/cm^2 was found, and for the imidazole system (undecylpyridine and octane), an average capacitance of 1.96 ±0.16 μF/cm^2 was found. Using a parallel plate model for the monolayer film, one obtains a thickness of 15.0 ± 1.9 Å for the pyridine-terminated system and 10.5 ± 0.9 Å for the imidazole-terminated system.[10] These distances are in reasonable agreement with expectation. Because the pyridine-terminated film consists mostly of undecanethiol and a small fraction of pyridine terminated material, the capacitance measurement should yield a film thickness that is similar to that expected for undecanethiol, perhaps slightly thicker. If one assumes that the alkanethiol chains are tilted at 30° from the surface normal,[11] one obtains a thickness of 12.3 Å for an undecanethiol film. A corresponding analysis for the imidazole terminated films, mostly composed of octanethiol, yields a film thickness of 9.0 Å.

Figure 2 illustrates the good blocking behavior observed for the mixed monolayer films. The three voltammograms in this figure were taken with the same redox solution (1 mM $[Fe(CN)_6]^{3-}$ /$[Fe(CN)_6]^{4-}$ in 0.5 M KCl) and the same parameters (cell geometry and 100 mV/s scan rate). The bare Au electrode shows a well-defined faradaic response (solid curve, a). In contrast, the voltammograms for the octanethiol and imidazole alkanethiol films (dashed curve, b) and the undecanethiol and pyridine−alkanethiol films (dotted curve, c) show the blocking behavior that is commonly found for insulating alkanethiol coated electrodes.[12] The blocking behavior indicates that the films are compact and inhibit penetration of the ferricyanide and ferrocyanide redox species. Because of the much larger size of a cytochrome *c*, as compared to ferricyanide and ferrocyanide, one expects no significant influence of defect sites on the observed faradaic current.

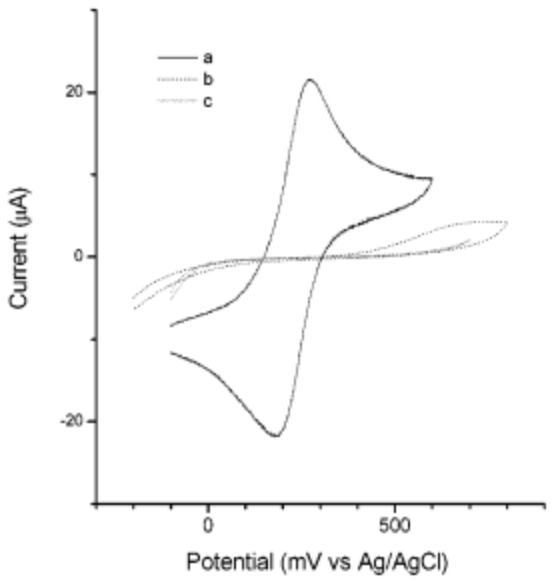

Figure 2. Voltammograms are shown for three different electrodes in contact with an equimolar $Fe(CN)_6^{3-/4-}$ solution (a, solid line is bare electrode; b, dashed line is imidazole mixed-film electrode; c, dotted line is pyridine mixed-film electrode).

Scanning tunneling microscopy studies were used to characterize the films. Figure 3A shows STM images of a pyridine terminated alkanethiol film to which cytochrome *c* had been immobilized. The bright spots show positions on the surface where the protein is adsorbed. The feature that is analyzed here occupies an area of about 15 nm^2 and a height of 0.7−0.9 nm. Although a bit larger than the cross-sectional area expected for individual cyctochrome *c* molecules (7−8 nm^2), this size is consistent with that expected for a protein.[13] A range of feature sizes, somewhat smaller than that shown and significantly larger ones, can be identified on the surface, however. An analysis of the image in Figure 3A indicates a surface coverage of ∼2.5%. It should be emphasized that the distribution of protein on the surface is not uniform; both regions with higher density of protein and with lower density of protein were readily identifiable. Figure 3B shows images of a monolayer film with no adsorbed protein (the scale is expanded over that shown in Figure 3A). Different regions are also evident in this image. Areas of depression (dark regions) are typically of dimension 20−30 Å across. Such structures represent depressions in the film that are associated with defects in the underlying Au surface and have been commonly observed for alkanethiol films on gold electrodes.[14] Although these features are interpreted as defects in the underlying gold, they are still coated with alkanethiol. In addition to this structure, elevated regions are also visible. These elevated regions, which are not present in pure alkanethiol monolayer films, correspond to 3−4% of the total area and are assigned to the pyridine-terminated thiols. The vertical/height length scale shown here for the images is compressed over the actual physical height. The reasons for this artificial compression when observing alkanethiols is discussed elsewhere.[15] It is evident from the image that the pyridine is not uniformly distributed throughout the film. The degree of “phase segregation” and its dependence on preparation and solvent conditions has not yet been investigated.

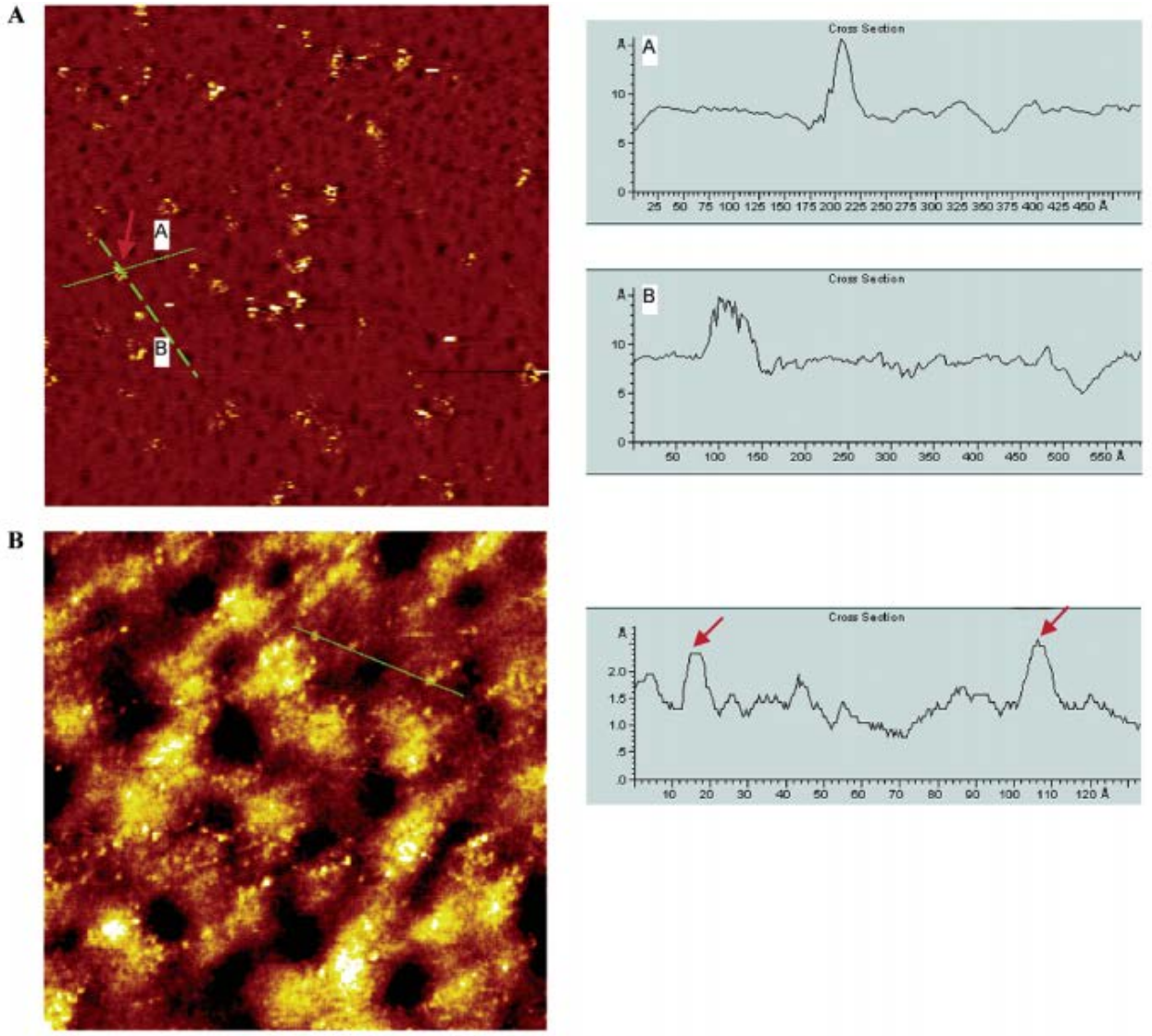

Figure 3. Panel A shows a topographic image for an electrode that has cytochrome *c* immobilized on the surface. A cross section through one of the features is shown for two different directions. The image size is 188 × 188 nm, the bias voltage is 0.5 V, and the current set point is 25 pA. Panel B shows an image for a pyridine-coated electrode with no cytochrome *c* adsorbed on the surface. The image size is 36.5 × 36.5 nm, the bias is 0.8 V, and the current set point is 0.1 nA.

Electrochemical Characterization. Cyclic voltammetry was performed on mixed monolayer films consisting of ~97% alkanethiol and 3% of an alkanethiol chain that was functionalized with either pyridine, imidazole, or nitrile.[16] These SAM-coated electrodes were incubated in a solution of cytochrome *c* for 30−60 min before being placed in a phosphate buffer solution at pH = 7.0. When the functionalized alkanethiol chain was longer than the alkanethiol diluent, cytochrome *c* was immobilized on the electrode surface. When the alkanethiol diluent was longer than the functionalized chain, the cytochrome *c* did not adsorb to the film. This conclusion was deduced from the inability to observe a faradaic current in the mixed films when the diluent alkanethiol had a chain length comparable to that of the ω-terminated thiol.

The electrochemical response was used to demonstrate that the cytochrome was immobilized on the surface of the monolayer film. Figure 4a shows voltammograms obtained for the imidazole

systems both with and without incubating the electrode in the cytochrome solution. In every case, when a monolayer-coated electrode was placed directly in the electrochemical cell containing only the buffer solution (not exposed to cytochrome *c*), the voltammogram displayed no faradaic response. Subsequently, this same electrode was treated with cytochrome *c*, rinsed, and placed in the buffer solution (see Experimental Section for details). In each case, a well-defined faradaic response was observed for the electrodes that were incubated in the cytochrome *c* solution. The same behavior was observed for the mixed films that were functionalized with pyridine, and voltammograms of this sort were shown for pyridine-terminated films earlier.[5]

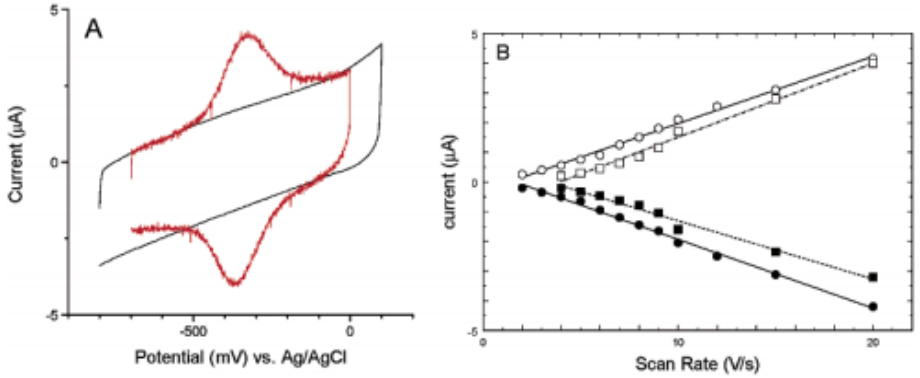

Figure 4. Panel A shows voltammograms for the imidazole films in which the surface has been exposed to cytochrome *c* and has not been exposed to cytochrome *c*. Panel B shows the linear dependence of the peak current on the voltage scan rate (imidazole is circles and pyridine is squares). The filled symbols are for the reduction wave, and the empty symbols are for the oxidation wave.

In addition to the incubation studies, the peak current, i_p, was measured as a function of the voltage scan rate for electrodes coated with cytochrome and was found to exhibit a linear dependence, which is consistent with immobilization of the cytochrome on the surface. These data are presented for both pyridine and imidazole in panel B of Figure 4. For a redox couple that is immobilized on the electrode surface, the peak current is given by

$$i_p = \frac{n^2F^2}{4RT}\upsilon N$$

where n is the number of electrons transferred, F is Faraday's constant, v is the voltage scan rate, and N is the number of redox active sites on the surface. For the imidazole system, the slope of the peak current versus scan rate plot, with $n = 1$, gives a surface coverage of $2.0 \pm 0.1 \times 10^{12}$ cm^{-2} (or $3.3 \pm 0.2 \times 10^{-12}$ mol/cm^2), and for the pyridine system, it gives $1.5 \pm 0.1 \times 10^{12}$ cm^{-2} (or $2.5 \pm 0.3 \times 10^{-12}$ mol/cm^2). The method for determining the electrode areas is described in the Experimental Section. The surface coverage of cytochrome was also determined by integrating the oxidation and reduction peaks of the voltammograms. This procedure generated coverages of $3.0 \pm 0.23 \times 10^{-12}$ mol/cm^2 for the imidazole system and $2.4 \pm 0.22 \times 10^{-12}$ mol/cm^2 for the pyridine system. The coverage calculated from the i_p dependence of the scan rate is consistent with the value obtained from the total charge transferred. Using the coverage of 1.5×10^{12} cm^{-2}cytochrome *c* on the pyridine-terminated monolayers, one calculates an average area per cytochrome *c* molecule of 67 nm^2, which is ~10 times the cross-sectional area of a cytochrome *c*molecule. Although these data do not quantify the homogeneity of the protein's

distribution on the surface, they indicate that the average distance between protein molecules is high.

The average coverage obtained from the electrochemical measurements, average of 10%, is significantly larger than that obtained from the STM image in Figure 3A (2.5%). Other regions of the surface were also imaged, and many of these had larger concentrations of protein features. In part, the difference between these two coverage measures can be accounted for by the limited sampling in a single STM image. In addition, it may be possible that the features do not all represent a single protein, but rather, two or more proteins might be clustered in regions of high pyridine concentration, and these clusters are not well-resolved. Other differences could arise from differences in the preparation and incubation of the monolayer films on the STM samples, as opposed to those on the Au ball electrodes (see Experimental Section).

It is possible to estimate the relative composition of the monolayers (e.g., percent pyridine-terminated alkanethiols, the active component, and alkanethiol, the diluent) from the STM data. The ratio of active alkanethiol to diluent in the solution used to prepare the mixed monolayer is 1:9. From Figure 3B, one determines ~3.3% for the coverage of pyridine by integrating the high points on the surface. Others have characterized the coverage of alkanethiol monolayer on polycrystalline gold and found it to be $\sim 7 \times 10^{-10}$ mol/cm^2.[17] Combining these values gives a surface concentration of $\sim 2.3 \times 10^{-11}$ mol/cm^2 for the pyridine-terminated thiol. The coverage of cytochrome *c* immobilized on the pyridine-terminated mixed monolayers determined from cyclic voltammetry (2.4×10^{-12} mol/cm^2) is about one-tenth of this value, or 1 cytochrome *c* for every 10 pyridines.

The voltammograms of the imidazole and pyridine mixed films at some selected voltage scan rates are presented in Figure 5. These data display well-defined peaks and show a small shift of the peak (oxidation)-to-peak (reduction) separation with the scan rate. This dependence can be used to analyze the electron-transfer rate constant (see below). It is evident that the noise level for the pyridine-terminated films (panel B) is higher than for the imidazole-terminated films (panel A). To obtain better defined peaks for the pyridine films at the slower scan rates, a filter (the time constant of the filter is 590 Hz) was used in the data collection. The use of a filter accounts for the difference in noise level between the slower scan rate curves and the higher scan rate curves, for which no filter was employed (in panel B). Table 1 reports the full width at half-maximum ($\Delta E_{1/2}$) of the reduction peak for the adsorbed cytochrome, and it is close to the ideal value of 91 mV for a fully reversible response. The peak widths for the mixed films are similar to that for dilute films of cytochrome *c* on carboxylic acid-terminated alkanethiols and indicate a high degree of homogeneity for the mixed systems. By contrast, an earlier study, which immobilized cytochrome *c*on pure layers of pyridine terminated alkanethiols, displayed significant broadening of the voltammograms and a large asymmetry between the oxidation and reduction responses[5]. For the electrodes where the cytochrome is freely diffusing, the difference between the voltammogram's peak potential and the half-peak potential is reported in Table 1. In this latter case, the ideal value should be 56 mV. The voltammograms for the nitrile films were significantly noisier than those shown here, and for this reason, the rest of the study focuses on the pyridine and imidazole mixed films.

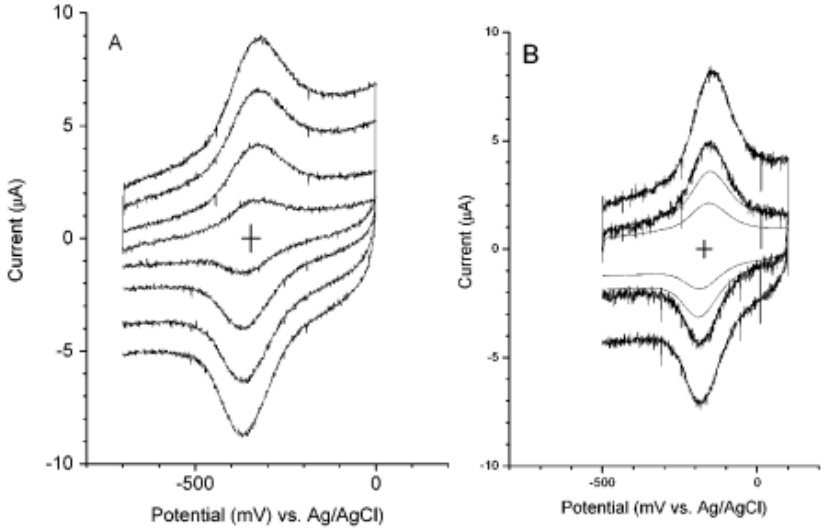

Figure 5. Voltammograms are shown for cytochrome *c* immobilized on the surface of mixed monolayer films containing imidazole functionalities (panel A) and pyridine functionalities (panel B). The scan rates for these voltammograms are 20 15, 10, and 6 V/s.

Table 1. Electrochemical Parameters for Different Electrode/ Cytochrome Systems

system	$E^{0\prime}$ (mV)	$\Delta E_{1/2}$ (mV)[a]	$\Delta E_{p/2}$ (mV)[b]	scan rate (V/s)
$HOC(CH_2)_6S$[c]	44 ± 2		58	0.2
$PyCO_2(CH_2)_2S$[c]	5		56	0.2
$HOOC(CH_2)_{10}S$	12 ± 3	99		0.6
$PyCO_2(CH_2)_{12}S/C_{11}H_{21}S$	−172 ± 10	108		1.0
$Im(CH_2)_{11}S/C_8H_{15}S$	−346 ± 20	117		1.0
$NC(CH_2)_{11}S/C_8H_{15}S$	−415 ± 20	132		8.0

[a] $\Delta E_{1/2}$ is full width at half max (fwhm) of a peak (that for the reduction peak is shown here). [b] $\Delta E_{p/2}$ is the difference between the peak potential and the half-peak potential (see 21). [c] In this system the cytochrome *c* is not immobilized on the electrode surface but is in solution at a concentration of 50 μM.

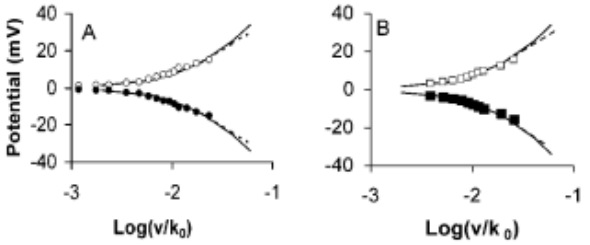

Figure 6. The dependence of the peak potential on the scan rate is shown for the imidazole system (panel A) and the pyridine system (panel B). The symbols follow the convention of Figure 4. Fits of the data to Marcus theory predictions are also shown for two different reorganization energies (0.8 eV is the solid line and 0.9 eV is the dashed line).

Table 1 also provides data on the apparent formal potentials for a number of different systems. For $S(CH_2)_2$−Py monolayers and hydroxyl-terminated monolayers to which the cytochrome does not adsorb, the reported formal potentials are 5 mV and 44 mV versus Ag/AgCl, respectively. For carboxylic acid-terminated monolayers to which the cytochrome is immobilized by electrostatic binding to the protein exterior, the apparent formal potential is 12 mV versus Ag/AgCl, intermediate between those found for the nonadsorbed protein. In contrast, for the mixed monolayer films, which are composed of pyridine, imidazole, and nitrile functionalities that can interact with the cytochrome's heme, a significant negative shift of the redox potential is observed, ranging from −172 mV for the pyridine system to −415 mV for the nitrile system. This shift in the redox potential is consistent with those found in homogeneous solution studies of cytochrome *c* when the ligands pyridine, imidazole, and nitrile are present.[18] Spectroscopic studies have shown that the pyridine, imidazole, and nitrile functionalities can bind to the redox center of the cytochrome in free solution.[19] Consequently, the negative shift in redox potential indicates an interaction between the terminal functionality of the layer and the cytochrome's heme.

The dependence of the reduction (or oxidation) peak's position on the voltage scan rate can be used to characterize the electron-transfer rate constant.[9,20] This method was used to determine rate constants for cytochrome *c* immobilized on the pyridine and imidazole terminated films.

Figure 6 shows a plot of the peak shift from apparent formal potential ($E_p - E^{0'}$) versus the voltage scan rate for each system, along with the best fit to the classical Marcus theory for the electron-transfer rate constant. The theoretical curves are shown for two different reorganization energies, 0.8 and 0.9 eV.[4] This procedure provides standard rate constants (k^0) of 780 s^{-1} for the pyridine-terminated layer (electron transfer through a C12 chain) and 850 s^{-1} for the imidazole-terminated layer (electron transfer through a C11 chain). The similar rates found for oxidation and reduction suggest a symmetry factor of 0.5 for the reaction.[21] These rate constants are quite high (peak voltage shifts are small), and one must be concerned about possible contributions from *iR* drop to the observed peak shifts.[7,21] To this end, the impedance of the electrochemical cell was measured to have a resistance of 300−500 Ω, which leads to a shift of <2 mV at the highest currents.

Association Strength. The strength of association and stability of the adsorbed cytochrome *c* films was assessed by monitoring the desorption kinetics. In this procedure, the coated film was placed in the solution, and within a few seconds (<10 s), a voltammogram was initiated with a scan rate of 20 V/s. Voltammograms were run at subsequent time points until the peak current was found to stabilize. Because the peak current is proportional to the amount of cytochrome adsorbed on the surface, this procedure generates a profile of the adsorbed species concentration as a function of time. Figure 7 shows these concentration profiles for both the imidazole and the pyridine-terminated films. The desorption kinetics can be modeled by considering that the system evolves toward an equilibrium of the following type

$$\mathrm{S{-}H_2O + Cyt.C} \underset{k}{\overset{k'}{\rightleftharpoons}} \mathrm{H_2O + S{-}Cyt.C}$$

where S−H_2O represents a solvated surface binding site, Cyt.C represents a cytochrome *c*molecule in solution, and S−Cyt.C represents a surface-bound cytochrome *c*. The rate constant *k*‘ characterizes the binding to surface sites, and the rate constant *k* characterizes the dissociation of the cytochrome from the binding site. Under the initial condition that all the cytochrome *c* is bound to the surface, one finds that the concentration of the surface adsorbed cytochrome θ(*t*) evolves according to

$$\frac{\theta(t)}{\theta(0)} = f + (1 - f)\exp(-(k + \kappa')t)$$

where κ‘ is given by *k*‘[Cyt.C], θ(*t*) is the coverage at time *t*, and *f* is the ratio κ‘/(θ(0)(κ‘ + *k*)). For the pyridine-terminated layer, the decay constant is 2.5 × 10^{-3} s^{-1}, and *f* is 0.14 ± 0.03, whereas the imidazole-terminated layer has a decay constant of 1.0 × 10^{-3} s^{-1} and f of 0.35 ± 0.04. The faster decay rate and the lower final value for the pyridine film indicates that its adsorption constant is smaller than that of the imidazole film; that is, the imidazole has a stronger association with the cytochrome than does the pyridine. If one assumes that θ(0) = 1, the fitting parameters give rate constants of *k* = 2.2 × 10^{-3} s^{-1} and κ‘ = 3.5 × 10^{-4} s^{-1} for pyridine, and *k* = 6.5 × 10^{-4} $s^{-1}$and κ‘ = 3.5 × 10^{-4} s^{-1} for imidazole. The effective association rate constant κ‘ appears to be the same for both systems, suggesting that the association is diffusion-limited. In contrast, the dissociation rate constants are different from one another, with the imidazole system being almost three times smaller than that of the pyridine system.

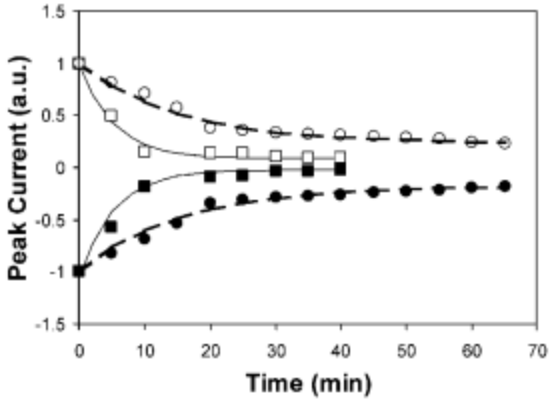

Figure 7. Time profiles for the surface concentration of immobilized cytochrome c are shown for both the pyridine-terminated films and the imidazole-terminated films. The symbol convention is the same as Figure 4.

DISCUSSION AND CONCLUSION

The immobilization of the cytochrome *c* on functionalized monolayer films is demonstrated through a combination of electrochemical and structural probes. By combining ω-terminated pyridine or imidazole alkanethiols with an alkanethiol diluent, it is possible to immobilize cytochrome *c* onto electrode surfaces through the interaction of the pyridine or imidazole with the heme of the cytochrome. The immobilization is demonstrated by the electrochemical observation that the peak current of the voltammogram grows linearly with the voltage scan rate and that the faradaic response is observed for the cytochrome *c* treated electrodes when they are immersed in the buffer solution. Complimentary studies used scanning tunneling microscopy to observe the presence of nanometer-scale objects on the surface of the monolayer film after they were treated in a solution containing cytochrome *c*. The lateral scale of the objects is similar to that expected for protein adsorption.

Previous work reported the immobilization of cytochrome *c* on the surface of pure monolayers of pyridinalalkanethiol. That work demonstrated the immobilization in a similar manner; however, the electrochemistry was not representative of a homogeneous distribution of redox sites. The pure monolayer films contained relatively broad peak widths (160−190 mV) and displayed asymmetric redox kinetics. In particular, the oxidation was found to be much faster than the rate constant for reduction. This observation was believed to reflect a change in the redox active sites after oxidation, associated with the degree, or strength, of interaction between the cytochrome and the pyridine. In contrast, the mixed monolayer systems show much narrower widths for the redox peaks (see Table 1) and yield similar rate constants for the reduction and oxidation waves. This indicates a much more uniform distribution of sites on the surface and not profound changes in binding geometry upon electron transfer.

The immobilization strategy utilized here is different from that used to immobilize the cytochrome *c*on the surfaces of −COOH-terminated alkanethiol monolayers. In that case, one observes similar widths for the voltammetric peaks, but the redox potentials observed on the COOH layers are much more positive than those found for the mixed monolayer films (see Table 1). The large difference in observed redox potential indicates that the nature of the immobilization is different in the two cases. The pyridine- and imidazole-terminated films have

redox potentials that are shifted negatively from that found for cytochrome *c* in free solution and are similar to the shift observed when cytochrome *c*/pyridine complexes are studied in free solution. In contrast, the COOH-terminated layer has a redox potential that is similar to that observed for cytochrome *c* in solution. These findings are consistent with the immobilization of cytochrome *c* on COOH-terminated films by adsorption on the protein's periphery, whereas the pyridine- and imidazole-terminated layers interact with the heme of the cytochrome.

The desorption of cytochrome *c* from the layer was monitored voltammetrically for both the pyridine-terminated layers and the imidazole-terminated layers. It was found that the dissociation of the cytochrome from the imidazole films is ∼3 times slower than that from the pyridine terminated films. This finding is consistent with a stronger interaction between the heme and the imidazole than with the heme and the pyridine.[18]

Finally, the electron-transfer rate constants were measured for the cytochrome *c* adsorbed on the film's surface. For the imidazole system, the rate constant was found to be 850 s^{-1} through a C11 methylene chain and 780 s^{-1} through a C12 methylene chain. These rate constants are comparable to rate constants observed for electron transfer through C6 methylene chains of carboxylic acid-terminated layers. A number of explanations are possible for this observation, such as changes in the reorganization energy, the electronic coupling, or the importance of local dipole fields. Currently, we are exploring these different issues, and our preliminary findings indicate that differences in the electronic coupling are likely to play a significant role in the final explanation. Detailed studies of the carboxylic acid-terminated films have identified an electron-transfer rate constant that is independent of distance for methylene chain lengths of C6 and shorter. The difference in length associated with C6 and C11 can be converted to a distance. If one takes the C−C bond length to be 1.5 Å and the alkane chains to be tilted at 30° from the surface normal, one finds a distance of 5.5 Å. This value is in reasonable agreement with the distance from the end of the COOH-terminated layer through the cytochrome *c* outer surface to the redox active heme, a tunneling distance of 5−6 Å, which is consistent with the COOH binding electrostatically to the cytochrome's outer surface. For the COOH-terminated monolayers, it has been reported that the cytochrome displays a tunneling dependence for methylene chain lengths of C9 and longer.[2,3] For the current system, one might expect that the range of distances, for which the electron-transfer rate constant is distance-independent, would be extended if the recognition element (pyridine, imidazole) binds to the heme of the protein rather than its outer surface. For longer methylene chains, one observes an exponential distance dependence for the electron-transfer rate.[22]

The ability to adsorb the redox active cytochrome *c* to the surface of SAM-coated gold electrodes in a restricted geometry has been demonstrated. These systems provide a model system to investigate aspects of electron-transfer dynamics between biomolecules and metal electrodes.

ACKNOWLEDGMENT

We acknowledge support in part from the U.S.−Israel BSF, the NSF−REU program at the University of Pittsburgh, and the Department of Energy. We thank D. Khoshtariya and E. Borguet for useful discussions.

REFERENCES

(1) (a) Lewis, N. S.; Wrighton, M. S. *Science* 1981, *211*, 944. (b) Armstrong, F. A.; Hill, H. A. O.; Walton, N. J. *Acc. Chem. Res.* 1988, *21*, 407.

(2) (a) Feng, Z. Q.; Imabayashi, S.; Kakiuchi, T.; Niki, K. *J. Chem. Soc., Faraday Trans.* 1997, *93*, 1 367. (b) Avilla, A.; Gregory, B. W.; Niki, K.; Cotton, T. M. *J. Phys. Chem. B* 2000, *104*, 2759.

(3) (a) Tarlov, M. J.; Bowden, E. F. *J. Am. Chem. Soc.* 1991, *113*, 1847. (b) Collinson, M.; Bosden, E. F.; Tarlov, M. J. *Langmuir*, 1992, *8*, 1247. (c) Song, S.; Clark, R. A.; Bowden, E. F.; Tarlov, M. J. *J. Phys. Chem*. 1993, *97*, 6564.

(4) Terrettaz, S.; Cheng, J.; Miller, C. J.; Guiles, R. D. *J. Am. Chem. Soc*. 1996, *118*, 7857.

(5) Yamamoto, H.; Liu, Haiying; Waldeck, D. H. *Chem. Commun.* 2001, 1032.

(6) Brutigan, D. L.; Ferguson, S.; Margoliash, E. *Methods in Enzymology*; Fleischer, S., Packer, L., Eds.; Academic Press: New York, 1978, Vol. 53, pp 131−132.

(7) Sawyer, D. T.; Sobkowiak, A.; Roberts, J. L., Jr. *Experimental Electrochemistry for Chemists*; Wiley: New York, 1995; pp 74−75. The diffusion constant of $Fe(CN)_6^{3-/4-}$ is assumed to be 7.63×10^{-6} cm^2/sec.

(8) Clavilier, J. *J..Electroanal. Chem*. 1980, *107*, 205.

(9) Napper, A. M.; Liu, H.; Waldeck, D. H.; *J. Phys. Chem. B* 2001, *105*, 7699.

(10) This calculation assumes a parallel plate model for the capacitance of the film ($C = \varepsilon$ (area)/(thickness)) and takes the alkanethiol dielectric constant ε to be 2.6.

(11) (a) Ulman, A. *Chem Rev.* 1996, *96*, 1533. (b) Schreiber, F. *Prog. Surf. Sci*. 2000,*65*, 151.

(12) (a) Miller, C. J. *Physical Electrochemistry: Principles, Methods, and Applications*; Rubinstein, I, Ed.; Marcel Dekker: New York, 1995; p 27. (b) Finklea, H. O. *Electroanalytical Chemistry*; Bard, A. J., Rubinstein, I., Eds. Marcel Dekker: New York, 1996; p 109. (c) Khoshtariya, D. E.; Dolidze, T. D.; Zusman, L. D.; Waldeck, D. H. *J. Phys. Chem.* 2001, *105*, 1818.

(13) *Cytochrome C: A Multidisciplinary Approach*; Scott, R. A., Mauk, A. G., Eds.; University Science Books: Sausalito, 1996.

(14) Poirier, G. E. *Chem. Rev.* 1997, *97*, 1117.

(15) (a) Weiss, P. S.; Bumm, L. A.; Dunbar, T. D.; Burgin, T. P.; Tour, J. M.; Allara, D. L. *Ann. N.Y. Acad. Sci.* 1998, *852*, 145. (b) Gorman, C. B.; Carrol, R. L.; He, Y.; Tian, F.; Fuierer, R. *Langmuir* 2000, *16*, 6312.

(16) Although the deposition solution contained a 9:1 ratio of thiol species, the STM studies indicate that the composition of the film deviates from this ratio significantly.

(17) Finklea, H. O. In *Encyclopedia of Analytical Chemistry*; Meyers, R. A., Ed.; John Wiley & Sons Ltd: Chichester, 2000.

(18) See Table 1 of Fedurco, M. *Coord. Chem. Rev*. 2000, *209*, 263, and references therein.

(19) (a) Spiro, T. G.; Li, X. Y. *Resonance Raman Spectra of Heme and Metalloproteins in Biological Applications of Raman Spectroscopy*; Wiley: New York, 1988 Vol. 3, p 1. (b) Hirota, S.; Ogura, T.; Shingawa, I. K.; Yoshikawa, S.; Kitagawa, T. *J. Phys. Chem.* 1996, *100*, 15274. (c) Yeh, S. R.; Rousseau, D. L. *J. Biol. Chem.* 1999, *274*, 17853. (d) Smith, M.; McLendon, G. *J. Am. Chem. Soc.* 1981, *103*, 4912. (e) Ferrer, J. C.; Gullemette, J. G.; Bogumil, R.; Inglis, S. C.; Smith, M.; Mauk, A. G. *J. Am. Chem. Soc.* 1993, *115*, 7507. (f) Liu, G.; Chen, Y. Tang. W. *J. Chem. Soc., Dalton Trans.* 1997, 795.

(20) (a) Tender, L.; Carter, M. T.; Murray, R. W. *Anal. Chem.* 1994, *66*, 3173. (b) Weber, K.; Creager, S. E. *Anal. Chem.* 1994, *66*, 3166. (c) Honeychurch, M. J. *Langmuir* 1999, *15*, 5158.

(21) (a) Bard, A. J.; Faulkner, L. R. *Electrochemical Methods;* Wiley: New York, 1980. (b) Bockris, J. O'M.; Reddy, A. K. N. *Modern Electrochemistry*; Plenum/Rosetta: New York, 1970.

(22) Wei, J.; Liu, H.; Khoshtariya, D.; Yamamoto, H.; Dick, A.; Waldeck, D. H. *Angew. Chem.*, submitted.